Composites Science and Technology 71 (2011) 666–673

Contents lists available at ScienceDirect

Composites Science and Technology

journal homepage: www.elsevier.com/locate/compscitech

Material tailoring for functionally graded hollow cylinders and spheres

G.J. Nie [a,*], Z. Zhong [a], R.C. Batra [b]

[a] School of Aerospace Engineering and Applied Mechanics, Tongji University, Shanghai 200092, China
[b] Department of Engineering Science and Mechanics, M/C 0219, Virginia Polytechnic Institute and State University, Blacksburg, VA 24061, USA

ARTICLE INFO

Article history:
Received 5 July 2010
Received in revised form 29 October 2010
Accepted 16 January 2011
Available online 23 January 2011

Keywords:
A. Functionally graded materials
B. Hollow cylinder and hollow sphere
B. Volume fractions of phases
C. Stress analysis
C. Material tailoring

ABSTRACT

We present a technique to tailor materials for functionally graded (FG) linear elastic hollow cylinders and spheres to attain through-the-thickness either a constant hoop (or circumferential) stress or a constant in-plane shear stress. The volume fractions of two phases of a FG material (FGM) are assumed to vary only with the radius and the effective material properties are estimated by using either the rule of mixtures or the Mori–Tanaka scheme; the analysis is applicable to other homogenization methods. For a FG cylinder we find the required radial variation of the volume fractions of constituents to make a linear combination of the radial and the hoop stresses uniform throughout the thickness. The through-the-thickness uniformity of the hoop stress automatically eliminates the stress concentration near the inner surface of a very thick cylinder. The through-the-thickness variations of Young's moduli obtained with and without considering the variation of Poisson's ratio are very close to each other for a moderately thick hollow cylinder but are quite different in a very thick hollow cylinder. For an FG sphere the required radial variation of the volume fractions of the two phases to get a constant circumferential stress is similar to that in an FG cylinder. The material tailoring results presented here should help structural engineers and material scientists optimally design hollow cylinders and spheres comprised of inhomogeneous materials.

1. Introduction

Functionally graded materials (FGMs) are composites composed of one or more phases spatially dispersed in a matrix of another phase. By controlling distributions of the volume fractions of phases within a body one can optimize structural performance and simultaneously meet other requirements. FGMs made of particulate composites have numerous interfaces and their ultimate strength is determined by the strength of these interfaces; e.g. see Love and Batra [1]. The interfaces between constituents can be eliminated or minimized when FGMs are fabricated by layering a molten mixture of two phases of different volume fractions. Various manufacturing techniques for FGMs have been discussed by [2,3].

Many investigators have studied deformations of FG structures by assuming that the macroscopic material properties are prescribed functions of the spatial coordinates. A challenging problem is to find the spatial variation of the constituent phases needed to attain a prescribed spatial distribution of stresses in a structure. The problem of designing an inhomogeneous orthotropic material to yield a desired spatial distribution of stresses has been studied by Leissa and Vagins [4] by assuming that all material moduli are proportional to each other. They found the spatial variation of the material elasticities to make either the hoop stress or the maximum in-plane shear stress uniform through the cylinder thickness. For designing FGMs with minimum thermal stresses, Tanaka et al. [5–7] developed a theoretical framework based on the direct sensitivity and the finite element methods. Sadagopan and Pitchumani [8–10] analyzed the optimal material tailoring problem by the combinatorial optimization technique, such as simulated annealing or genetic algorithms, in conjunction with analytical microstructure–property relations. Tanigawa et al. [11] used the nonlinear programming method to find the material composition for minimizing transient thermal stresses induced in an infinitely long inhomogeneous plate. Vinogradov [12] studied the effectiveness of material tailoring in asymmetric laminated beam-columns to enhance their buckling resistance. It is found that the performance of laminates can be controlled through a proper selection of the number, the stacking sequence and the material properties of the layers. Cho and Ha [13,14] presented an efficient and reliable optimization procedure to ascertain the volume-fraction distribution for relaxing or minimizing the steady-state effective thermal stresses in heat-resisting FGMs. Cho and Choi [15] found the volume-fraction distribution in an elastic–plastic metal-ceramic FGM by considering the variation of its yield stress with the volume fraction of the constituents. Batra and Jin [16] determined the fiber orientation in each ply of a laminated composite plate to optimize its natural frequencies.

* Corresponding author.
E-mail address: ngj@tongji.edu.cn (G.J. Nie).

0266-3538/$ - see front matter © 2011 Elsevier Ltd. All rights reserved.
doi:10.1016/j.compscitech.2011.01.009

Qian and Batra [17] employed a meshless method and a higher-order shear and normal deformable plate theory to compute the spatial variation of the volume fractions of constituents to optimize natural frequencies of a cantilever plate. Love and Batra [18] numerically computed the effective thermal and mechanical properties of a particulate composite composed of elasto-plastic inclusions imbedded in an elastic–plastic matrix. Goupee and Vel [19,20] used a meshless method to study two-dimensional thermo-mechanical deformations of a FG structure and employed a genetic algorithm to optimize the spatial distribution of the constituent phases. Sun and Hyer [21] delineated the improvement in the axial buckling load by continuously varying the fiber orientation angle in an elliptic fiber-reinforced composite cylinder. Batra [22–23] determined the radial variation of the shear modulus in Hookean and Mooney–Rivlin cylinders and spheres so that either the hoop stress or the in-plane shear stress is uniform during their axisymmetric deformations. Nie and Batra [24] found the required radial variation of the shear modulus for a linear combination of the radial and the hoop stresses to have a preassigned variation in a cylinder made of an incompressible FGM. They also determined the radial variation of either Young's modulus or Poisson's ratio for a cylinder to have either uniform in-plane shear stress or uniform hoop stress [25] during axisymmetric deformations. Na and Kim [26–28] optimized the volume fractions of constituents in a flat and a stepped FG panel to reduce stresses and improve their thermo-mechanical buckling behavior.

Works cited above indicate that one can improve the performance of structures through material tailoring. Here we analytically find the spatial variation of the volume fractions of phases required to make a linear combination of the hoop and the radial stresses constant through-the-thickness of a cylinder or a sphere. For an FGM composed of spherical inclusions imbedded in a matrix, the volume fractions of constituents are evaluated by either the rule of mixtures or the Mori–Tanaka scheme [29–32]. We note that Vel and Batra [33] have compared stress and displacement fields in an FG plate with effective material properties derived by using the Mori–Tanaka and the consistent schemes. Our computed values of the volume fractions of constituents depend upon the homogenization technique employed to derive values of effective material parameters of the FGM from that of constituents. We note that Charalambakis [34] has recently reviewed various homogenization techniques.

2. Formulation of the problem

2.1. Cylinder

Consider an infinitely long FG hollow cylinder with inner radius r_{in}, outer radius r_{ou}, and its inner and outer surfaces subjected,

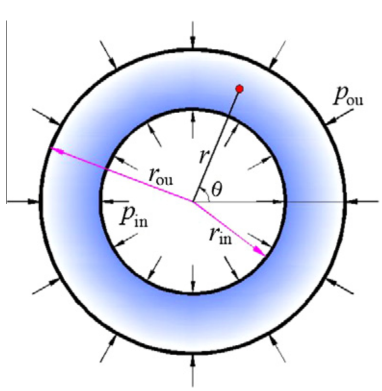

Fig. 1. Section of an infinitely long FG hollow cylinder.

respectively, to pressures p_{in} and p_{ou}, as shown in Fig. 1. We assume that an axisymmetric plane strain state of deformation prevails in the cylinder, and describe its deformations in cylindrical coordinates (r, θ) with the origin at the center of a cross-section of the cylinder. Thus the material composition varies only in the thickness direction and not in the axial direction. The problem of finding the composition as a function of all three coordinates is considerably more challenging than the one studied here. For the present problem, the compatibility equation in terms of infinitesimal strains ε_{rr} and $\varepsilon_{\theta\theta}$ is

$$\frac{d}{dr}(r\varepsilon_{\theta\theta}) - \varepsilon_{rr} = 0. \tag{1}$$

In the absence of body forces the equation of equilibrium is

$$\frac{d\sigma_{rr}}{dr} + \frac{\sigma_{rr} - \sigma_{\theta\theta}}{r} = 0, \tag{2}$$

where σ_{rr} and $\sigma_{\theta\theta}$ are the radial and the circumferential (or the hoop) stresses respectively. The boundary conditions on the inner and the outer surfaces of the cylinder are

$$\sigma_{rr}(r_{in}) = -p_{in}; \quad \sigma_{rr}(r_{ou}) = -p_{ou}. \tag{3a, b}$$

Constitutive equations for a linear elastic isotropic FGM with radial inhomogeneity are

$$\begin{aligned} \varepsilon_{rr} &= \frac{1}{E_1(r)}[\sigma_{rr} - \nu_1(r)\sigma_{\theta\theta}], \\ \varepsilon_{\theta\theta} &= \frac{1}{E_1(r)}[\sigma_{\theta\theta} - \nu_1(r)\sigma_{rr}], \end{aligned} \tag{4a, b}$$

where

$$E_1(r) = \frac{E(r)}{1 - \nu^2(r)}, \quad \nu_1(r) = \frac{\nu(r)}{1 - \nu(r)}, \tag{5a, b}$$

$E(r)$ and $\nu(r)$ are Young's modulus and Poisson's ratio, respectively, and they are functions of the radial coordinate, r. Henceforth we call E_1 and ν_1 the effective Young's modulus and the effective Poisson's ratio, respectively.

2.2. Sphere

For a hollow sphere with material properties varying only in the radial direction and loaded by hydrostatic pressures on the inner and the outer surfaces, it is reasonable to assume that a material point moves only in the radial direction. Eq. (1) is the compatibility equation, and the equilibrium equation in spherical coordinates for an axisymmetric problem is

$$\frac{d\sigma_{rr}}{dr} + \frac{2}{r}(\sigma_{rr} - \sigma_{\theta\theta}) = 0. \tag{6}$$

The boundary conditions on the inner and the outer surfaces of the sphere are the same as those listed in Eq. (3). Constitutive equations for a linear elastic isotropic FGM with radial inhomogeneity are

$$\begin{aligned} \varepsilon_{rr} &= \frac{1}{E(r)}[\sigma_{rr} - 2\nu(r)\sigma_{\theta\theta}], \\ \varepsilon_{\theta\theta} &= \frac{1}{E(r)}[\sigma_{\theta\theta} - \nu(r)(\sigma_{rr} + \sigma_{\theta\theta})]. \end{aligned} \tag{7a, b}$$

3. Homogenization of material properties

For an FGM made of two distinct isotropic materials, for example, a metal and a ceramic, the rule of mixtures gives the following effective material properties

$$E(r) = [1 - \xi(r)]E_m + \xi(r)E_p, \quad \nu(r) = [1 - \xi(r)]\nu_m + \xi(r)\nu_p, \tag{8a, b}$$

where it has been tacitly assumed that the FGM is also isotropic; our analysis will also apply to a cylinder whose material is transversely isotropic with the cylinder axis as the axis of transverse isotropy. Alternatively, one can use the Mori–Tanaka scheme to arrive at

$$K(r) = K_m + \frac{\xi(r)(K_p - K_m)(3K_m + 4G_m)}{3K_m + 4G_m + 3(1 - \xi(r))(K_p - K_m)}, \tag{9a}$$

$$G(r) = G_m + \frac{\xi(r)(G_p - G_m)(5G_m(3K_m + 4G_m))}{5G_m(3K_m + 4G_m) + 6(1 - \xi(r))(K_m + 2G_m)(G_p - G_m)}, \tag{9b}$$

$$E(r) = \frac{9G(r)K(r)}{G(r) + 3K(r)}, \quad \nu(r) = \frac{3K(r) - 2G(r)}{2G(r) + 6K(r)}, \tag{9c}$$

where $\xi(r)$ equals the volume fraction of the inclusion (i.e., phase 1), suffixes m and p denote the matrix and the inclusion, respectively, and $K(r)$ and $G(r)$ the bulk and the shear moduli, respectively. We note that the moduli $E(r)$ and $\nu(r)$ should satisfy the Hashin–Shtrikman upper and lower bounds [35] and the material moduli given by the Mori–Tanaka scheme are lower bounds. Other homogenization techniques have been reviewed in [34] and our computed through-the-thickness variations of the volume fractions of constituents depend upon the homogenization technique employed.

4. Stress fields in homogeneous cylinders and spheres

In view of the boundary conditions in Eq. (3), we solve simultaneously Eqs. (1), (2) and (4) and then stresses in a hollow cylinder made of a homogeneous material can be obtained as

$$\begin{aligned} \sigma_{rr} &= \frac{p_{in} r_{in}^2 - p_{ou} r_{ou}^2}{r_{ou}^2 - r_{in}^2} + \frac{(p_{ou} - p_{in}) r_{ou}^2 r_{in}^2}{r^2 (r_{ou}^2 - r_{in}^2)}, \\ \sigma_{\theta\theta} &= \frac{p_{in} r_{in}^2 - p_{ou} r_{ou}^2}{r_{ou}^2 - r_{in}^2} + \frac{(p_{in} - p_{ou}) r_{ou}^2 r_{in}^2}{r^2 (r_{ou}^2 - r_{in}^2)}. \end{aligned} \tag{10a, b}$$

The expressions of stresses in Eq. (10) are the same as those given in [22].

Similarly, we can get the expressions of stresses in a hollow sphere composed of a homogeneous material,

$$\begin{aligned} \sigma_{rr} &= \frac{p_{in} r_{in}^3 - p_{ou} r_{ou}^3}{r_{ou}^3 - r_{in}^3} + \frac{(p_{ou} - p_{in}) r_{ou}^3 r_{in}^3}{r^3 (r_{ou}^3 - r_{in}^3)}, \\ \sigma_{\theta\theta} &= \frac{p_{in} r_{in}^3 - p_{ou} r_{ou}^3}{r_{ou}^3 - r_{in}^3} + \frac{(p_{in} - p_{ou}) r_{ou}^3 r_{in}^3}{2r^3 (r_{ou}^3 - r_{in}^3)}. \end{aligned} \tag{11a, b}$$

It is clear that the hoop stress varies through the cylinder and the sphere thickness. For the hollow cylinder loaded on the inner surface only, the hoop stress is maximum on the inner surface and minimum on the outer surface. Thus if the cylinder is designed based on the maximum principal stress or the maximum in-plane shear stress reaching a critical value, then the material through the cylinder thickness will not be optimally utilized. One can draw the same conclusion for the sphere, and the cases when both the cylinder and the sphere are loaded by a pressure on the outer surface.

5. Material tailoring for cylinders

5.1. Stress fields

From the standpoint of macromechanical failure theories for brittle and ductile materials, it is desirable to have either the maximum principal stress or the maximum shear stress constant in the cylinder. We now find the spatial distribution of constituents to achieve

$$k\sigma_{rr} + \sigma_{\theta\theta} = C_0, \tag{12}$$

through the cylinder thickness. In Eq. (12) k is a prescribed constant, and the constant C_0 is related to pressures applied on the inner and the outer surfaces, and the radii of the inner and the outer surfaces of the hollow cylinder. For $k = 0\,(-1)$ in Eq. (12), the hoop stress (the in-plane shear stress) is constant through the cylinder thickness. Assuming that $k \neq -1$, we substitute from Eq. (12) into Eq. (2), integrate the resulting equation with respect to r and get

$$\sigma_{rr} = \frac{C_0}{k+1} + C_1 r^{-k-1}, \quad \sigma_{\theta\theta} = \frac{C_0}{k+1} - kC_1 r^{-k-1}, \tag{13a, b}$$

where C_1 is a constant to be determined. We follow a similar procedure for finding stresses when $k = -1$. Using boundary conditions listed as Eq. (3a,b), the radial and the hoop stresses for $k \neq -1$ and $k = -1$, respectively, can be expressed as

$$\sigma_{rr} = \frac{(p_{in} - p_{ou}) r_{in}^{k+1} r_{ou}^{k+1} r^{-k-1} + p_{ou} r_{ou}^{k+1} - p_{in} r_{in}^{k+1}}{r_{in}^{k+1} - r_{ou}^{k+1}}, \tag{14a}$$

$$\sigma_{\theta\theta} = \frac{k(p_{ou} - p_{in}) r_{in}^{k+1} r_{ou}^{k+1} r^{-k-1} + p_{ou} r_{ou}^{k+1} - p_{in} r_{in}^{k+1}}{r_{in}^{k+1} - r_{ou}^{k+1}}, \tag{14b}$$

and

$$\sigma_{rr} = \frac{(p_{ou} - p_{in}) \ln r - p_{ou} \ln r_{in} + p_{in} \ln r_{ou}}{\ln r_{in} - \ln r_{ou}}, \tag{15a}$$

$$\sigma_{\theta\theta} = \frac{(p_{ou} - p_{in}) \ln r - p_{ou} \ln r_{in} + p_{in} \ln r_{ou} + p_{ou} - p_{in}}{\ln r_{in} - \ln r_{ou}}. \tag{15b}$$

Thus the problem reduces to finding $E(r)$ and $\nu(r)$ (alternatively, the volume fraction of constituents) such that stresses are given by Eqs. (14) and (15) rather than by Eq. (10).

5.2. Material tailoring for hollow cylinders

Substitution for normal strains from Eq. (4a,b) into Eq. (1) gives the equation

$$\begin{aligned} &(\sigma_{\theta\theta} - \sigma_{rr})[1 - \nu_1(r)] + \frac{r}{E_1(r)} \frac{dE_1(r)}{dr} [\sigma_{rr} \nu_1(r) - \sigma_{\theta\theta}] \\ &\quad - r\sigma_{rr} \frac{d\nu_1(r)}{dr} + r\frac{d\sigma_{\theta\theta}}{dr} - r\nu_1(r)\frac{d\sigma_{rr}}{dr} = 0. \end{aligned} \tag{16}$$

for the determination of $E_1(r)$ and $\nu_1(r)$. Substitution for stresses from Eqs. (14) or (15), and for $E_1(r)$ and $\nu_1(r)$ either from Eq. (8) or from Eq. (9) into Eq. (16) gives a nonlinear first-order ordinary differential equation for the volume fraction $\xi(r)$ of the inclusion which we numerically integrate with respect to r by using the Runge–Kutta method.

As an example, we consider a FG hollow cylinder composed of silicon carbide (SiC) and aluminum (Al), and the inner and the outer surfaces subjected to uniform pressures. We take E_{Al} = 73 GPa, E_{SiC} = 450 GPa, ν_{Al} = 0.33, and ν_{SiC} = 0.16. For a prescribed value of $\xi(r_{in})$ the volume fraction $\xi(r)$ of SiC particulates is determined from the nonlinear equation for $\xi(r)$.

5.2.1. Effect of different homogenization techniques

Consider a moderately thick cylinder with r_{in} = 60 mm, r_{ou} = 100 mm, p_{in} = 100 MPa and p_{ou} = 0 MPa. With the effective material properties of the FGM evaluated by the rule of mixtures and for the hoop stress to be constant in the cylinder, the required variation with the radius of the volume fraction of SiC particulates is computed under the condition of $\xi(r_{in}) = 0.0$. The polynomial function obtained by fitting through these discrete values by the least squares method is

$$\xi(r) = 0.0038444r - 0.229528, \quad 60\ \text{mm} \leqslant r \leqslant 100\ \text{mm}. \tag{17}$$

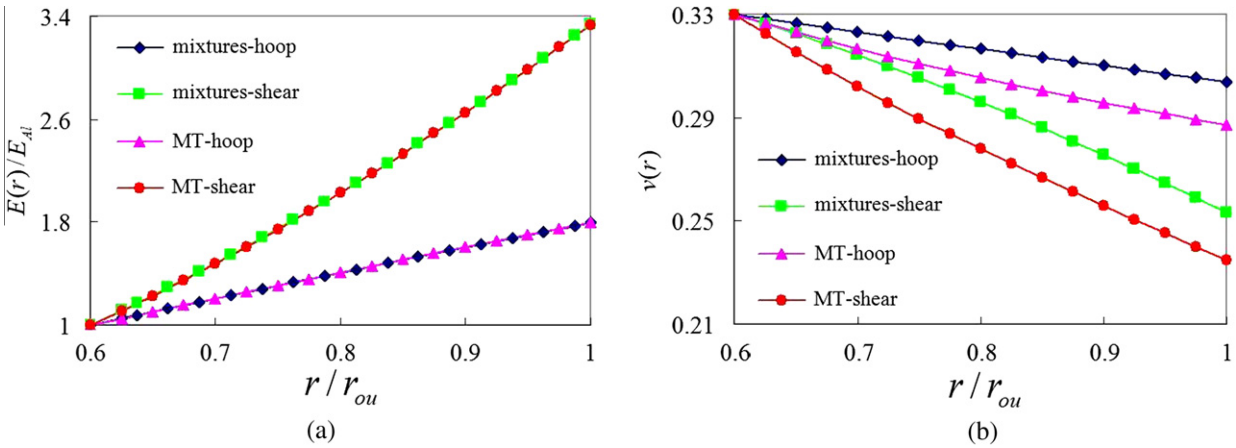

Fig. 2. The required variations of: (a) Young's modulus and (b) Poisson's ratio to achieve a constant hoop stress and a constant in-plane shear stress in a FG hollow cylinder with uniform pressures applied to its inner and outer surfaces.

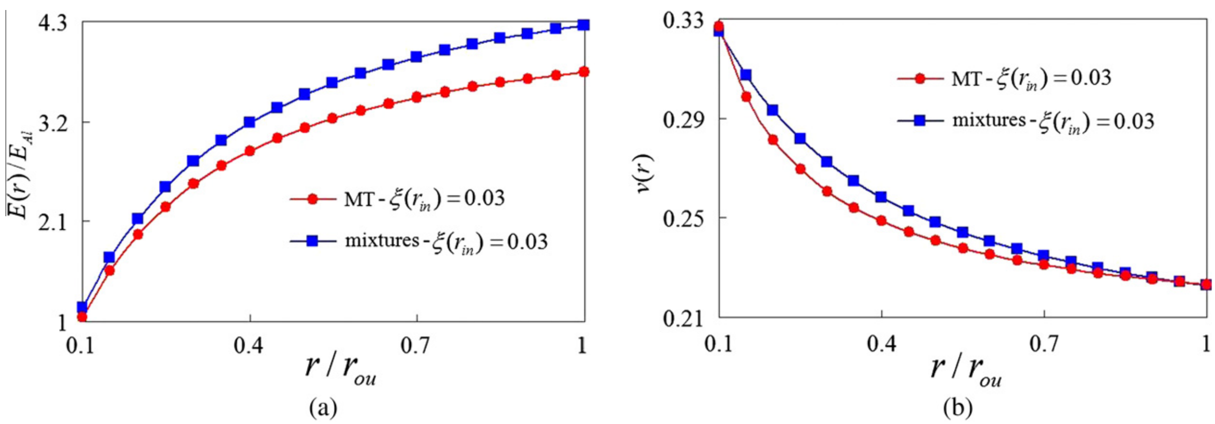

Fig. 3. For r_{in}/r_{ou} = 0.1 and the two homogenization techniques, the required variations of: (a) Young's modulus and (b) Poisson's ratio to achieve a constant hoop stress in an FG cylinder.

Following the same procedure as above, for the in-plane shear stress to be constant in the cylinder we get

$$\xi(r) = 0.0000655r^2 + 0.000865r - 0.28818,\quad 60\ \text{mm} \leqslant r \leqslant 100\ \text{mm}. \tag{18}$$

When the effective material properties of the cylinder are derived by using the Mori–Tanaka scheme, the analogues of Eqs. (17) and (18), respectively, are

$$\xi(r) = -0.000086r^2 + 0.0233524r - 1.0904,\quad 60\ \text{mm} \leqslant r \leqslant 100\ \text{mm}, \tag{19}$$

and

$$\xi(r) = -0.00023206r^2 + 0.05547233r - 2.489869,\quad 60\ \text{mm} \leqslant r \leqslant 100\ \text{mm}. \tag{20}$$

The corresponding variations of Young's modulus and Poisson's ratio for a constant hoop stress and a constant in-plane shear stress computed from Eqs. (8) and (9) are exhibited in Fig. 2. In Fig. 2, 'mixtures' and 'MT' represent, respectively, solutions obtained by using the rule of mixtures and the Mori–Tanaka scheme, and 'hoop' and 'shear' denote, respectively, a constant hoop stress and a constant in-plane shear stress in the cylinder. It is observed from results plotted in Fig. 2a that the variation of Young's modulus with the radius for the hoop stress to be constant through the cylinder thickness is nearly linear; this agrees with the earlier result of Nie and Batra [25]. In order to achieve a constant in-plane shear stress, Young's modulus and Poisson's ratio must have relatively steep variations from the inner to the outer surfaces of the cylinder. Young's modulus needs to increase quickly and Poisson's ratio needs to decrease from the inner to the outer surfaces. Furthermore,

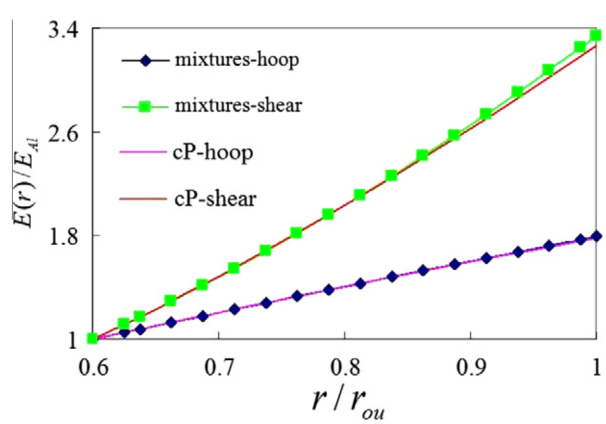

Fig. 4. The required variation of Young's modulus computed with and without considering the variation of Poisson's ratio for the hoop stress and the shear stress to be constant through the cylinder thickness.

we note that the required variation of Young's modulus with the radius to achieve the same stress field is nearly the same for the two homogenizations methods. However, the required variation of Poisson's ratio to achieve the same stress state depends upon the homogenization scheme.

As mentioned in the Introduction, for a very thick cylinder stress concentration near the inner surface can be eliminated by suitably tailoring the volume fractions of phases. We now consider an Al/SiC FG cylinder with $r_{in}/r_{ou} = 0.1$, $r_{ou} = 100$ mm, $p_{in} = 0$, and $p_{ou} = 100$ MPa. For the two homogenization techniques and for the hoop stress to be a constant in a very thick cylinder, the required variations of Young's modulus and Poisson's ratio with the radius are shown in Fig. 3. We note that values of the effective Young's modulus increase rapidly at points adjacent to the inner surface of the cylinder, and then almost affinely. However, the value of Poisson's ratio should monotonically decrease with an increase in r to attain a constant hoop stress in the cylinder, and eliminate stress concentration near the inner surface of the cylinder. It is found that for the two homogenization techniques values of Young's modulus on the outer surface of the cylinder differ by about 13% and the maximum difference in the values of Poisson's ratio occurs at a point in the cylinder interior. As mentioned earlier other homogenization techniques will give different variations of the volume fractions of the two constituents. Only physical tests can decide which homogenization technique gives reasonable values of the effective moduli over the range of interest.

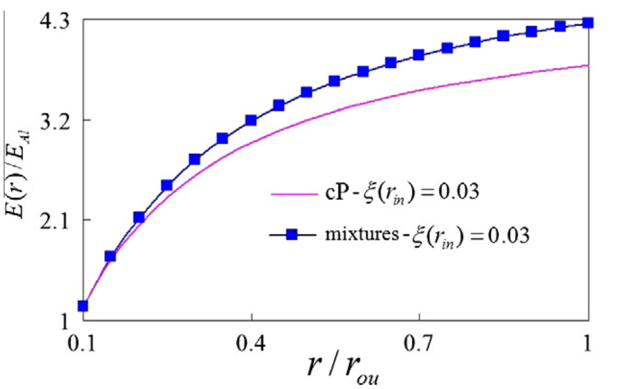

Fig. 5. For $r_{in}/r_{ou} = 0.1$, the required variation of Young's modulus computed with and without considering the variation of Poisson's ratio for the hoop stress to be constant through the cylinder thickness.

5.2.2. Effect of the variation of Poisson's ratio

For a moderately thick cylinder with $r_{in} = 60$ mm, $r_{ou} = 100$ mm, $p_{in} = 100$ MPa, $p_{ou} = 0$ MPa, and $\xi(r_{in}) = 0.0$ we investigate the effect of the variation of Poisson's ratio. It is assumed that Poisson's ratio is constant through the cylinder thickness and we compute Young's modulus by using the rule of mixtures. For Poisson's ratio of the composite equal to that of the matrix, the through-the-thickness variation of Young's modulus is exhibited in Fig. 4; results for Poisson's ratio obtained by the rule of mixtures are also plotted in Fig. 4 for comparison purposes. The curves represented by 'cP-' in Fig. 4 are solutions obtained by setting Poisson's ratio equal to that of the matrix. It is clear that the two variations of $E(r)$ are very close

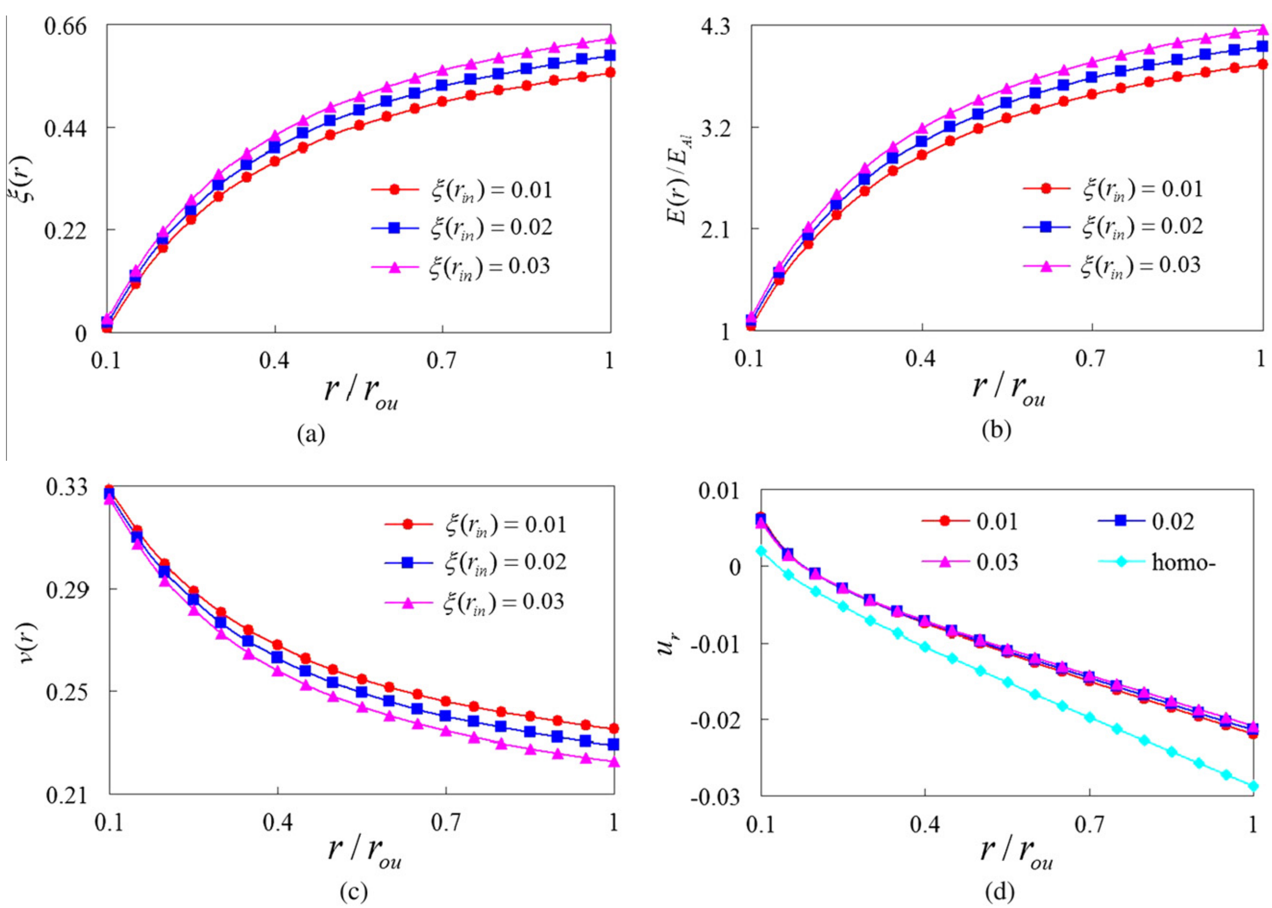

Fig. 6. For $r_{in}/r_{ou} = 0.1$ and three values of the volume fraction of SiC on the inner surface, the required through-the-thickness variations of: (a) the volume fraction of SiC, (b) Young's modulus, and (c) Poisson's ratio to achieve a constant hoop stress and the corresponding variation of (d) the radial displacement in an FG cylinder.

to each other implying thereby that the variation of Poisson's ratio with the radius has little effect on the required variation of Young's modulus to achieve a given stress state for a moderately thick hollow FG cylinder.

Results for the required variations of Young's modulus obtained with and without considering the variation of Poisson's ratio in a very thick cylinder are exhibited in Fig. 5. Consider the very thick cylinder with $r_{in}/r_{ou} = 0.1$, *rou* = 100 mm, $p_{in} = 0$, and $p_{ou} = 100$ MPa. It is seen that two values of Young's modulus on the outer surface of the cylinder differ by about 14%. By comparing results plotted in Fig. 5 with those shown in Fig. 4, we conclude that the influence of the variation of Poisson's ratio on the required variation of Young's modulus to achieve a constant hoop stress in the cylinder is greater for a cylinder with $r_{in}/r_{ou} = 0.1$ than that for a cylinder with $r_{in}/r_{ou} = 0.6$.

5.2.3. Effect of different values of material properties on the inner surface

For an Al/SiC FG cylinder with $r_{in}/r_{ou} = 0.1$, $r_{ou} = 100$ mm, $p_{in} = 0$, and $p_{ou} = 100$ MPa we now consider the effect of different values of the volume fraction of SiC assigned on the inner surface of the cylinder. For the hoop stress to be constant in the cylinder, the computed variations of the volume fraction and the corresponding Young's modulus and Poisson's ratio based on the rule of mixtures are displayed in Fig. 6. Different variations of volume fractions of phases give the same stress field evincing thereby that the inverse problem does not have a unique solution. However, as depicted in Fig. 6d, the displacement field for the three different volume fractions differs from that in a homogeneous cylinder with Young's modulus and Poisson's ratio equal to their average values of the two phases, Al and SiC.

6. Material tailoring for hollow spheres

6.1. Stress fields

For a hollow sphere we analyze the problem for

$$\sigma_{\theta\theta} = C_0, \tag{21}$$

where C_0 is related to pressures applied on the inner and the outer surfaces and their radii. Substituting from Eq. (21) into Eq. (6) and considering the boundary conditions listed in Eq. (3a,b), we get

$$\sigma_{rr} = \frac{(p_{ou}r_{ou}^2 - p_{in}r_{in}^2)r^2 + (p_{in} - p_{ou})r_{in}^2 r_{ou}^2}{(r_{in}^2 - r_{ou}^2)r^2}, \tag{22a}$$

$$\sigma_{\theta\theta} = \frac{p_{in}r_{in}^2 - p_{ou}r_{ou}^2}{r_{ou}^2 - r_{in}^2}. \tag{22b}$$

6.2. Material tailoring for spheres

Substitution for the strains from Eq. (7) into Eq. (1) and for stresses from Eq. (22) into the resulting equation, we arrive at the following ordinary differential equation for finding $E(r)$ and $\nu(r)$:

$$(\sigma_{\theta\theta} - \sigma_{rr})[1 + \nu(r)] + \frac{r}{E(r)}\frac{dE(r)}{dr}[(\sigma_{rr} + \sigma_{\theta\theta})\nu(r) - \sigma_{\theta\theta}]$$
$$-r(\sigma_{rr} + \sigma_{\theta\theta})\frac{d\nu(r)}{dr} - r\nu(r)\frac{d\sigma_{rr}}{dr} + r[1 - \nu(r)]\frac{d\sigma_{\theta\theta}}{dr} = 0. \tag{23}$$

For an Al/SiC FG sphere with $p_{in} = 0$, $p_{ou} = 100$ MPa, $r_{ou} = 100$ mm, and $\xi(r_{in}) = 0.01$, the computed radial variations of the volume fraction of SiC in three spheres with $r_{in}/r_{ou} = 0.1$, $r_{in}/r_{ou} = 0.3$, and

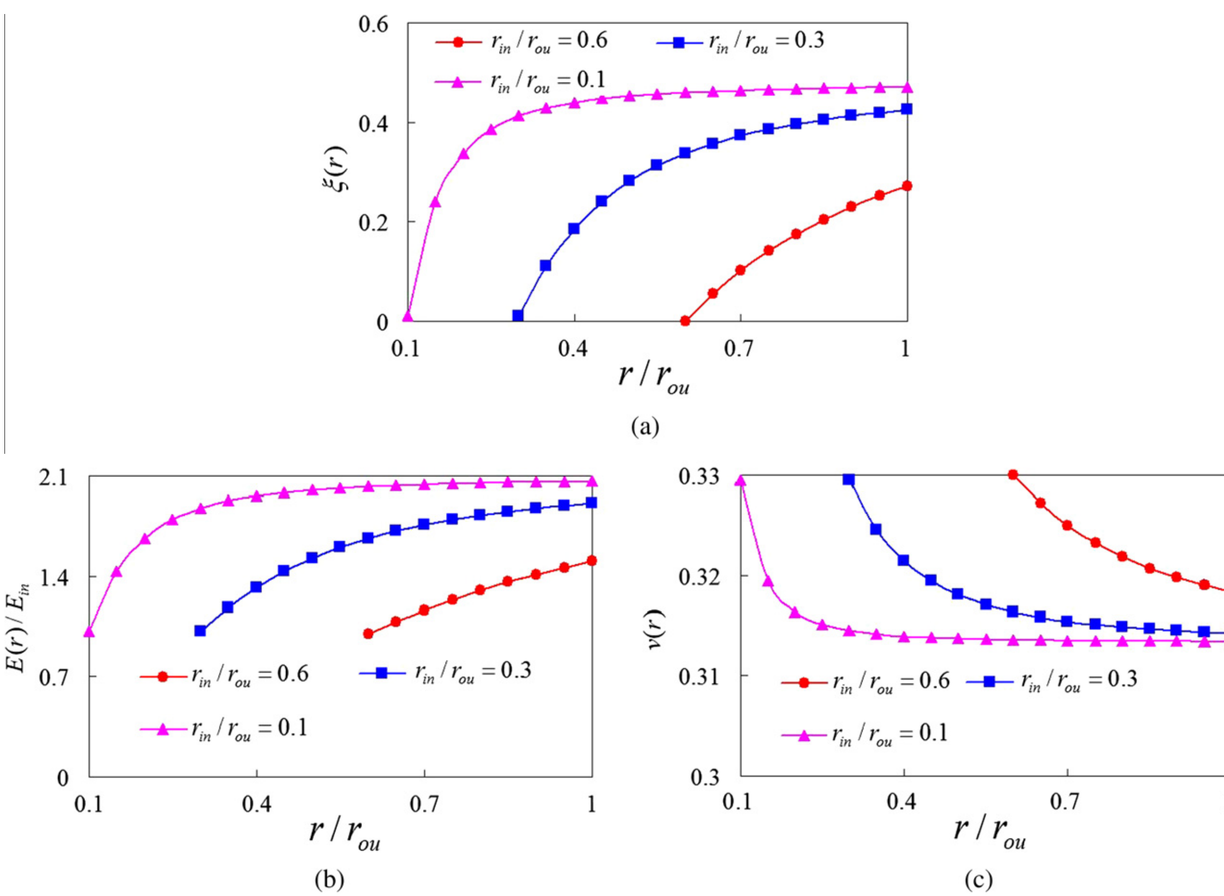

Fig. 7. The required variations of: (a) the volume fraction of SiC, (b) Young's modulus and (c) Poisson's ratio to achieve constant circumferential stress in three FG spheres.

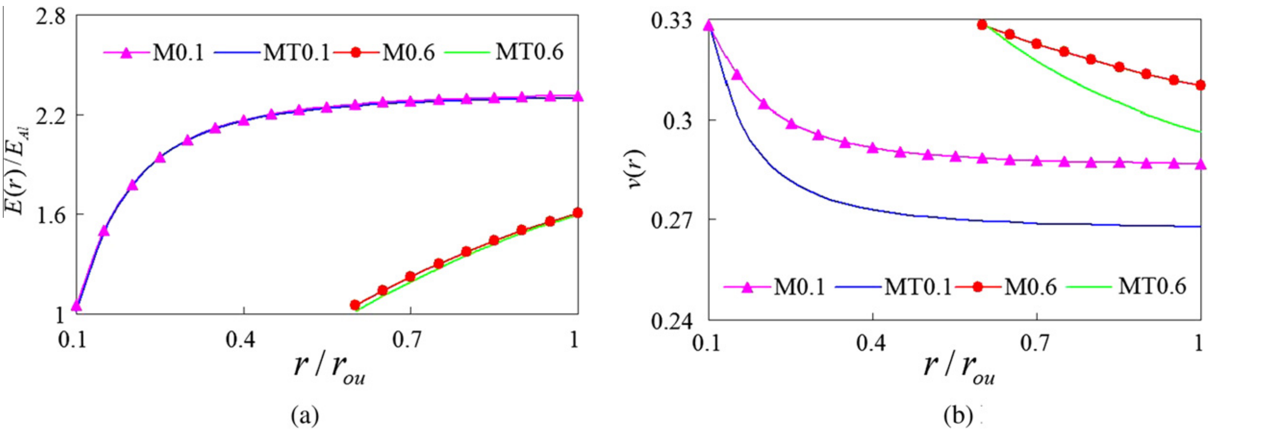

Fig. 8. For the two homogenization schemes the required variations of: (a) Young's modulus and (b) Poisson's ratio to achieve constant circumferential stress in two FG spheres.

$r_{in}/r_{ou} = 0.6$ for the circumferential stress to be constant are exhibited in Fig. 7a. Here the rule of mixtures has been used to determine the effective material properties and through-the-thickness variations of Young's modulus and Poisson's ratio obtained from Eq. (8) are shown in Fig. 7b and c. Comparing results exhibited in Fig. 7 with those plotted in Figs. 2 and 5, it is seen that the required variations of Young's modulus and Poisson's ratio are qualitatively similar for a cylinder and a sphere. For the sphere with $r_{in}/r_{ou} = 0.1$, the stress concentration near the inner surface can be effectively eliminated by varying the volume fractions of the two constituents. For the hollow sphere with $r_{in}/r_{ou} = 0.6$, the variation of Young's modulus with the radius is nearly linear. We recall that for a sphere made of an incompressible FGM Batra [22] found that for the circumferential stress to be constant in the sphere the shear modulus must vary linearly with the radius.

For the two homogenization techniques the required variations of Young's modulus and Poisson's ratio with the radius to attain a constant circumferential stress in a sphere are compared in Fig. 8. The curves marked 'M0.1' and 'M0.6' represent results obtained by using the rule of mixtures and for $r_{in}/r_{ou} = 0.1$ and 0.6, respectively. Similarly curves labeled 'MT0.1' and 'MT0.6' represent results obtained with the Mori–Tanaka scheme. Note that the homogenization technique strongly affects the variation of Poisson's ratio with the radius but has a little influence on values of Young's modulus.

By using the rule of mixtures to derive the effective material properties, we have compared in Fig. 9 results obtained by considering the variation of Poisson's ratio to those when Poisson's ratio is constant and equals that of the matrix. The curves represented by 'cP-' are solutions for the constant Poisson's ratio, and '0.1'(or '0.6') denotes the value of r_{in}/r_{ou}. It is found that the spatial variation of Poisson's ratio strongly affects the spatial variation of $E(r)$ for the sphere with $r_{in}/r_{ou} = 0.1$ but has a little effect for the sphere with $r_{in}/r_{ou} = 0.6$. The maximum difference in the two values of $E(r)$ for the sphere with $r_{in}/r_{ou} = 0.1$ is nearly 10%.

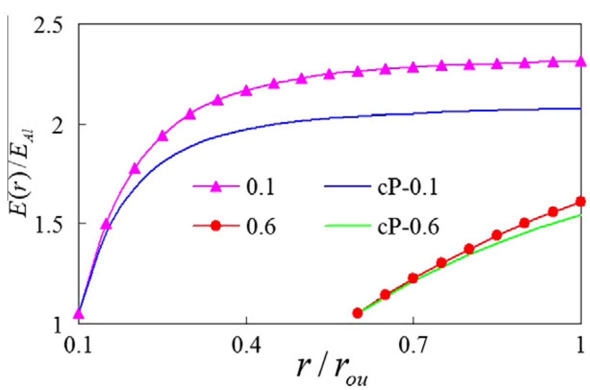

Fig. 9. The required variation of Young's modulus computed with and without considering the variation of Poisson's ratio for the circumferential stress to be constant in two FG spheres.

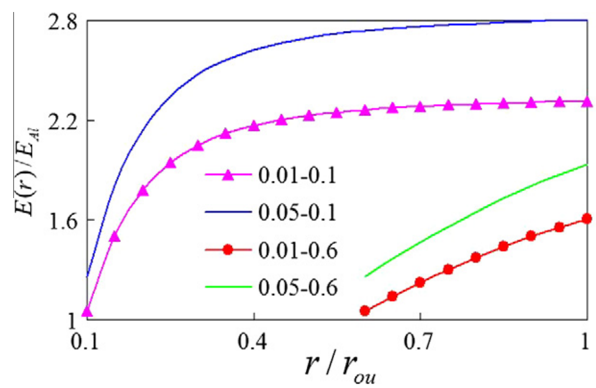

Fig. 10. The required variations of Young's modulus to achieve a constant circumferential stress in two FG spheres with different values of the volume fraction of SiC on their inner surfaces.

For two different values of the volume fraction of SiC particulates on the inner surface of a sphere, the computed required variations of Young's modulus to achieve the same constant circumferential stress are compared in Fig. 10. Curves labeled '0.01–' (or '0.05–') represent results for $\xi(r_{in}) = 0.01$ (or 0.05) and '0.1' (or '0.6') denotes the ratio r_{in}/r_{ou}. As for the cylinder problem studied above, it is seen that different values of $\xi(r_{in})$ can attain the same stress field within a sphere; however the corresponding displacements will be different.

7. Conclusions

We have studied the tailoring of volume fractions of constituents in FG hollow cylinders and spheres to achieve either through-the-thickness uniform hoop (or circumferential) stress or in-plane shear stress. For a cylinder, we have found the radial variation of the volume fraction of the constituents to have a linear combination of the radial and the hoop stresses constant through the cylinder thickness. Thus by suitably varying the composition, one can eliminate the stress concentration near the inner surface of a thick FG cylinder. It is found that the two homogenization techniques, namely the rule of mixtures and the Mori–Tanaka scheme, generally have a small (large) influence on the computed spatial variation of Young's modulus (Poisson's ratio). It is reasonable to conclude that the computed radial variations of the volume fractions of the two phases will depend upon the homogenization technique used. The through-the-thickness variations of Young's moduli obtained with and without considering the variation of Poisson's ratio are very close to each other for a moderately thick hollow cylinder but are quite different in a very thick hollow cylinder. In order to have a uniform circumferential stress through the sphere thickness, the radial variations of Young's modulus and Poisson's ratio are similar to those for a hollow cylinder.

The present findings should help structural engineers and material scientists optimally design inhomogeneous cylinders and spheres.

Acknowledgments

This work was supported by the Specialized Research Fund for the Doctoral Program of Higher Education (No. 20070247029) and the National Natural Science Foundation of China (Nos. 10872150 and 11072177). RCB's work was partially supported by the Office of Naval Research Grant N00014-1-06-0567 to Virginia Polytechnic Institute and State University. Views expressed in the paper are those of authors and neither of the funding agencies nor or their Institutions.

References

[1] Love BM, Batra RC. Effect of particulate/matrix debonding on the formation of adiabatic shear bands. Int J Mech Sci 2010;52:386–97.
[2] Liu T, Wang W, Gao A, Zhang C, Wang C, He J. Fabrication of functionally graded materials by a semi-solid forming process under magnetic field gradients. Acta Mater 2007;57:992–5.
[3] Watanabe Y, Inaguma Y, Sato H, Miura-Fujiwara E. A novel fabrication method for functionally graded materials under centrifugal force. The centrifugal mixed-powder method. Materials 2009;2:2510–25.
[4] Leissa AW, Vagins M. The design of orthotropic materials for stress optimization. Int J Solids Struct 1978;14:517–26.
[5] Tanaka K, Tanaka Y, Enomoto K, Poterasu VF, Sugano Y. Design of thermoelastic materials using direct sensitivity and optimization methods: reduction of thermal stresses in functionally gradient materials. Comput Methods Appl Mech Eng 1993;106:271–84.
[6] Tanaka K, Tanaka Y, Watanabe H, Poterasu VF, Sugano Y. An improved solution to thermoelastic material design in functionally gradient materials: scheme to reduce thermal stresses. Comput Methods Appl Mech Eng 1993;109:377–89.
[7] Tanaka K, Watanabe H, Sugano Y, Poterasuc VF. A multicriterial material tailoring of a hollow cylinder in functionally gradient materials: scheme to global reduction of thermoelastic stresses. Comput Methods Appl Mech Eng 1996;135:369–80.
[8] Sadagopan D, Pitchumani R. Property-based optimal tailoring of composite materials. Phys Prop Compos 1996:1–10.
[9] Sadagopan D, Pitchumani R. A combinatorial optimization approach to composite materials tailoring. J Mech Des 1997;119:494–503.
[10] Sadagopan D, Pitchumani R. Application of genetic algorithms to optimal tailoring of composite materials. Compos Sci Technol 1998;58:571–89.
[11] Tanigawa Y, Matsumoto M, Akai T. Optimization of material composition to minimize thermal stresses in nonhomogeneous plate subjected to unsteady heat supply. JSME Int J, Ser A 1997;40(1):84–93.
[12] Vinogradov AM. Material tailoring effects on buckling of asymmetric laminated beam-columns. J Adv Mater 1999;31(2):3–8.
[13] Cho JR, Ha DY. Optimal tailoring of 2D volume-fraction distributions for heat-resisting functionally graded materials using FDM. Comput Methods Appl Mech Eng 2002;191:3195–211.
[14] Cho JR, Ha DY. Volume fraction optimization for minimizing thermal stress in NiAl2O3 functionally graded materials. Mater Sci Eng A 2002;334(1–2):147–55.
[15] Cho JR, Choi JH. A yield-criteria tailoring of the volume fraction in metal-ceramic functionally graded material. Eur J Mech A/Solids 2004;23:271–81.
[16] Batra RC, Jin J. Natural frequencies of a functionally graded rectangular plate. J Sound Vibr 2005;282:509–16.
[17] Qian LF, Batra RC. Design of bidirectional functionally graded plate for optimal natural frequencies. J Sound Vibr 2005;280:415–24.
[18] Love BM, Batra RC. Determination of effective thermomechanical parameters of a mixture of two thermoviscoplastic constituents. Int J Plast 2006;22:1026–61.
[19] Goupee AJ, Vel SS. Two-dimensional optimization of material composition of functionally graded materials using meshless analyses and a genetic algorithm. Comput Methods Appl Mech Eng 2006;195:5926–48.
[20] Goupee AJ, Vel SS. Multi-objective optimization of functionally graded materials with temperature-dependent material properties. Mater Des 2007;28:1861–79.
[21] Sun M, Hyer MW. Use of material tailoring to improve buckling capacity of elliptical composite cylinders. AIAA J 2008;46(3):770–82.
[22] Batra RC. Optimal design of functionally graded incompressible linear elastic cylinders and spheres. AIAA J 2008;46(8):2050–7.
[23] Batra RC. Material tailoring and universal relations for axisymmetric deformations of functionally graded rubberlike cylinders and spheres. Math Mech Solids, in press.
[24] Nie GJ, Batra RC. Material tailoring and analysis of functionally graded isotropic and incompressible linear elastic hollow cylinders. Compos Struct 2010;92:265–74.
[25] Nie GJ, Batra RC. Exact solutions and material tailoring for functionally graded hollow circular cylinders. J Elast 2010;99:179–201.
[26] Na KS, Kim JH. Optimization of volume fractions for functionally graded panels considering stress and critical temperature. Compos Struct 2009;89:509–16.
[27] Na KS, Kim JH. Volume fraction optimization of functionally graded composite panels for stress reduction and critical temperature. Finite Elements Anal Des 2009;45(11):845–51.
[28] Na KS, Kim JH. Volume fraction optimization for step-formed functionally graded plates considering stress and critical temperature. Compos Struct 2010;92(6):1283–90.
[29] Mori T, Tanaka K. Average stress in matrix and average elastic energy of materials with misfitting inclusions. Acta Metall 1973;21:571–4.
[30] Benveniste Y. A new approach to the application of Mori–Tanaka's theory in composite materials. Mech Mater 1987;6:147–57.
[31] Kikuaki T, Watanabe H, Sugano Y, Poterasuc VF. A multicriterial material tailoring of a hollow cylinder in functionally gradient materials: scheme to global reduction of thermoelastic stresses. Comput Methods Appl Mech Eng 1996;135:369–80.
[32] Cheng ZQ, Batra RC. Three-dimensional thermoelastic deformations of a functionally graded elliptic plate. Composites: Part B 2000;31:97–106.
[33] Vel SS, Batra RC. Exact solutions for thermoelastic deformations of functionally graded thick rectangular plates. AIAA J 2002;40:1421–33.
[34] Charalambakis N. Homogenization techniques and micromechanics. A survey and perspectives. Appl Mech Rev 2010;63:030803.
[35] Hashin Z, Shtrikman S. A variational approach to the theory of the elastic behavior of multiphase materials. J Mech Phys Solids 1963;13:213–22.